A Nature Portfolio journal



https://doi.org/10.1038/s42003-025-08833-v

Hypomethylation of thrombospondin-1 promoter region is associated with reduced aqueous humor flow

Check for updates

Kit Ying Choy^{1,2}, Wei-ying Yang ¹, Choi-ying Ling¹, King-kit Li¹, Hoi Lam Li³, Hong-lok Lung⁴, Chi-ho To^{1,2,5,6}, Chi Wai Do^{1,2,5,7}, W. Daniel Stamer^{8,9} & Samantha Sze-wan Shan ^{1,2,5} □

Prolonged use of dexamethasone (DEX) elevates intraocular pressure (IOP) and increases the risk of developing glaucoma. In a previous study, we demonstrate that DEX stimulates the expression of thrombospondin-1 (THBS1) in primary human trabecular meshwork (hTM) cells, and that inhibiting THBS1 expression prevents DEX-induced elevation of IOP in mice. Therefore, we investigate the mechanism by which DEX regulates THBS1 expression. Treatment with the DNA methylation inhibitors, 5-azacytosine (5-AC) or 5-aza-2'-deoxycytidine (5-aza-dC), upregulates THBS1 protein levels in vitro and in vivo, reduces outflow facility in perfused mouse eyes, and elevates IOP in mice. In primary hTM cells, 7-day DEX treatment results in hypomethylation of the THBS1 promoter region and reduces transcript levels of 2 DNA methyltransferases (DNMTs), DNMT1 and DNMT3A. Taken together, we show that DEX reduces expression of DNMTs and DNA methylation of the THBS1 promoter region, supporting a critical role for THBS1 in DEX-induced outflow reduction.

Glaucoma is a leading cause of blindness worldwide and is commonly referred to as the thief of sight. It is characterized by optic neuropathy and the loss of retinal ganglion cells, resulting in permanent blindness. Elevated IOP is a major risk factor for glaucoma¹. Other risk factors for glaucoma include high myopia^{2–5}, aging^{6–9}, and use of corticosteroids¹⁰. Corticosteroids, including DEX and prednisolone (PRED), are known to increase IOP^{11,12}, and prolonged treatment with corticosteroids has been shown to trigger glaucomatous optic neuropathy¹³. Elevated IOP is the result of decreased outflow capacity at the level of the trabecular meshwork (TM) and Schlemm's canal, the primary route for the egress of aqueous humor¹⁰. Hence, the TM is thought to play an important role in the regulation of IOP¹⁴.

THBS1 is an matricellular extracellular matrix (ECM) protein localized¹⁵ and synthesized¹⁶ at the TM of human eyes. DEX and PRED have been shown to alter the alpha-actin cytoskeletal architecture of primary hTM cells^{17,18} and to increase protein expression of THBS1¹⁹. THBS1 is a major activator of latent transforming growth factor beta 1 (TGFB1)^{19,20} and regulates many cellular activities, including cell adhesion, ECM remodeling and cell migration²¹. In our previous study, we showed that Rho-associated

protein kinase (ROCK) inhibitor Y39983-mediated downregulated THBS1 at the mRNA and protein levels²², suggesting that THBS1 expression was regulated by ROCK activity. In addition, we demonstrated that a THBS1 inhibitory peptide and siRNA-mediated knockdown of THBS1 significantly increased the outflow facility in mouse eyes. These findings strongly suggest that reduced THBS1 expression may be a key cellular event for increasing outflow facility, reducing IOP, and potentially for glaucoma pathogenesis²².

DEX alters DNA methylation at multiple promoter regions of genes with corresponding changes in mRNA expression in hTM cells²³, suggesting that DNA methylation may also play a role in steroid-induced glaucoma. DNA methylation is an epigenetic process in which DNMT1, DNMT3A, and DNMT3B add methyl groups to cytosine groups in genomic DNA, to create 5-methylcytosine²⁴. Junemann et al. showed altered levels of genomic DNA methylation in peripheral blood mononuclear cells of patients with primary open-angle glaucoma (POAG) relative to controls patients²⁵. The *THBS1* gene was shown to be hypomethylated in glaucomatous Schlemm's canal endothelial cells²⁶. Hence, epigenetic modification is a potential mechanism through which DEX may regulate gene expression in TM cells and IOP. Therefore, we tested the hypothesis that hypomethylation of the

¹School of Optometry, The Hong Kong Polytechnic University, Hong Kong, China. ²Centre for Eye and Vision Research (CEVR), 17W Hong Kong Science Park, Hong Kong, China. ³Ophthalmology, Boston University Chobanian & Avedisian School of Medicine, Boston, MA, USA. ⁴Department of Chemistry, Hong Kong Baptist University, Hong Kong, China. ⁵Research Centre for SHARP Vision (RCSV), The Hong Kong Polytechnic University, Hong Kong, China. ⁶School of Optometry and Vision Sciences, Cardiff University, Cardiff, UK. ⁷Research Institute of Smart Ageing (RISA), The Hong Kong Polytechnic University, Hong Kong, China. ⁸Department of Ophthalmology, Duke University, Durham, NC, USA. ⁹Department of Biomedical Engineering, Duke University, Durham, NC, USA. □ e-mail: samantha.shan@polyu.edu.hk

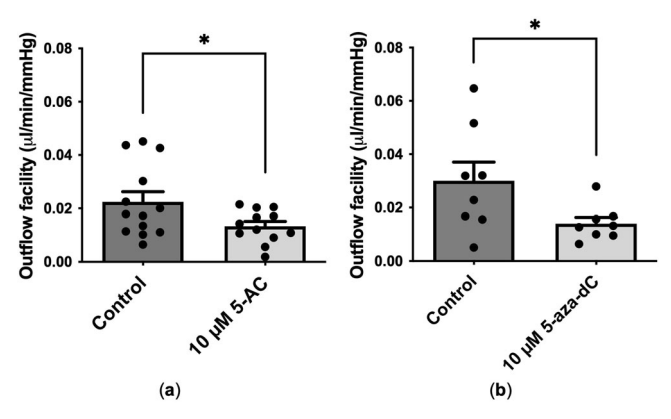


Fig. 1 | DNA methylation inhibitors reduced outflow facility of mouse eyes ex vivo. a 5-AC (n = 12) reduced the outflow facility by 40%, when compared to vehicle-control mouse eyes (n = 13). b 5-aza-dC (n = 8) reduced outflow facility by 53% when compared to vehicle-control mouse eyes (n = 8). Data are represented as mean \pm SEM. *P < 0.05 (Student's t test).

THBS1 gene is a key mechanism through which corticosteroids induce ocular hypertension and POAG. Here, we have shown in hTM cells that DEX indeed reduces methylation of the *THBS1* promoter region, and this change is consistent with DEX-mediated increases in THBS1 protein levels, leading to the reduced outflow facility ex vivo and increased IOP in vivo adult male C57BL/6 J mice, a popular animal model for ocular research due to several ocular anatomical and physiological similarities to humans, such as the conventional outflow pathway^{27,28}.

Results

DNA methylation inhibitors decreased outflow facility ex vivo

To study the effects of DNA methylation inhibitors on outflow facility of mouse eyes, we enucleated both eyes from adult male C57BL/6 J mice and perfused them with or without 5-AC or 5-aza-dC, while outflow facility was measured under constant pressure. Both 5-AC and 5-aza-dC are cytosine analogues and DNMT inhibitors to promote global DNA hypomethylation and gene expression. After 4 h of perfusion, 10 μ M of 5-AC reduced the outflow facility of the treated eyes by 40% (P = 0.0451), when compared to the fellow control eyes (Fig. 1a). Similarly, 10 μ M of 5-aza-dC also reduced the outflow facility of the treated eyes by 53% (P = 0.0470; Fig. 1b).

DNA methylation inhibitors increased IOP in vivo

Since the outflow facility determines IOP, we next studied the effects of DNA methylation inhibitors on IOP of mice. For each of the adult C57BL/6 J mouse, one eye was randomly selected for either 5-AC or PBS topical administration, while another eye was left untreated as control. The treatments were thrice a day for 14 days, and IOP was monitored. As the topically applied drug has lower capacity to penetrate the cornea, a higher dose (50 μ M) of 5-AC was used in the in vivo experiments relative to the in vitro experiments. Topical application of 5-AC induced a significant IOP elevation from day-13 (P=0.0113; Fig. 2a). At day-15, 5-AC induced a significant IOP elevation by 2.85 \pm 0.89 mmHg (P=0.0007) in 5-AC-treated eyes, when compared to PBS-treated eyes (Fig. 2b). After the topical administration, 5-AC increased the IOP by 1.76 \pm 0.71 mmHg (P=0.0045), when compared to baseline (Fig. 2b). This demonstrated that repeated administration of DNA methylation inhibitors elevated IOP of mouse eyes in vivo.

DNA methylation inhibitors induced THBS1 expression

We next examined the effects of DNA methylation inhibitors on THBS1 expression in vivo and in vitro. After 14-day topical application of 5-AC or PBS, mouse eyes were carefully enucleated, cryosectioned, and immunostained against THBS1. Figure 3a showed that 5-AC topical application induced THBS1 expression at TM when compared to PBS-treated eye. Similarly, 2-day treatment of 5-AC resulted in an upregulation of *THBS1*

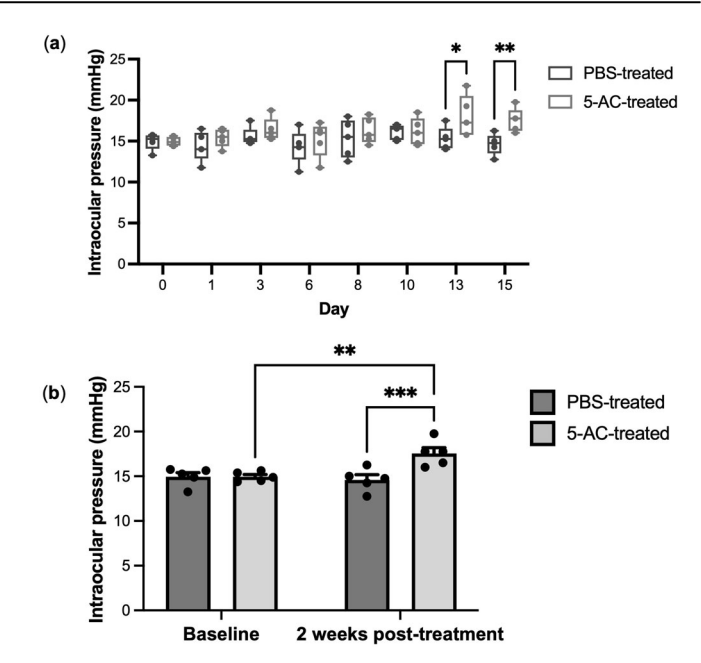


Fig. 2 | 5-AC elevated IOP of adult C57BL/6 J mice. a 5-AC (n=5) or PBS (n=5) was topically administrated onto adult C57BL/6 J mouse eyes thrice a day for 14 days and IOP was monitored every 2-3 days. Data are represented as a box contains the 25th to 75th percentiles of dataset. The center line represents the median value while the whiskers extend from the box to the smallest and largest values of the dataset. b At day-15, 5-AC (n=5) significantly increased IOP by 2.85 \pm 0.89 mmHg when compared to PBS-treated eyes (n=5). It also significantly increased the IOP by 1.76 \pm 0.71 mmHg when compared to baseline. Data are represented as mean \pm SEM. *P < 0.05, **P < 0.01 and ***P < 0.001 (two-way repeated measures ANOVA followed by Bonferroni's multiple comparisons test).

gene expression level in hTM cells (Fig. 3b). These indicated that THBS1 expression was tightly regulated by DNA methylation.

DEX induced hypomethylation at THBS1 promoter region

In hTM cells, DEX-induced changes of promoter region methylation status and gene expression have been shown for multiple genes, but not for THBS1 ²³. To understand whether the DEX-induced THBS1 upregulation in hTM cells observed in our previous study¹⁷ is due to changes in DNA methylation, we analysed the DNA methylation status at the *THBS1* promoter region using methylation specific PCR (MSP). Only unmethylated *THBS1* products, but not methylated *THBS1* products, were observed in DEX-treated samples (Fig. 4, lower panel). Both unmethylated and methylated THBS1 products were observed in vehicle-control samples (Fig. 4, upper panel). The results indicated that DEX treatment induced DNA hypomethylation at the *THBS1* promoter region.

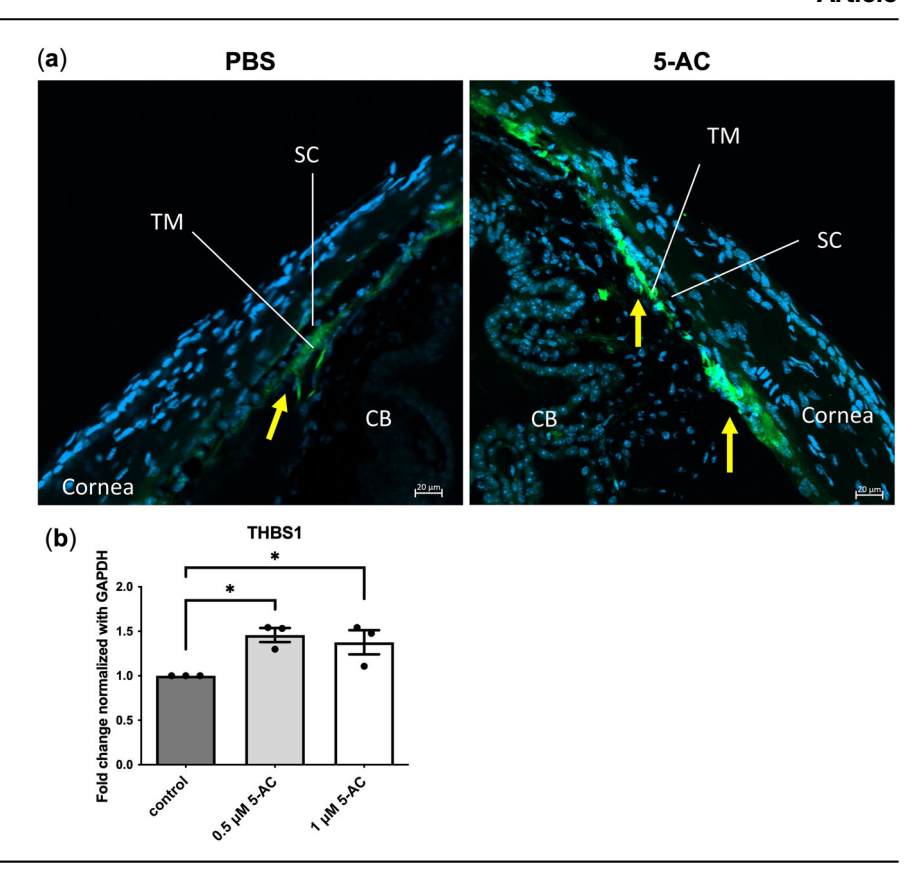
DEX downregulated DNMT1 and DNMT3A gene expressions

To understand whether the DEX-induced aberrant methylation of THBS1 was associated with changes in the expression of DNMTs, we analysed the gene expression levels of DNMT1, DNMT3A, and DNMT3B, as they are the generally recognized forms of DNMTs in mammals which perform the genomic methylation²⁹. DEX reduced transcript levels of DNMT1 and DNMT3A by 40% (P=0.0426) and 55% (P=0.0021), respectively, but not of DNMT3B (Fig. 5). This suggested that DEX may reduce DNA methylation at certain promoter regions in hTM cells by lowering DNMT expression.

DEX induced DNA methylation changes in hTM cells

To identify the overall methylation patterns in 3 individual hTM cell strains in response to DEX treatment, genomic DNA extracted from DEX-treated and vehicle-control hTM cells were sequenced using whole genome bisulfite

Fig. 3 | THBS1 was upregulated after 5-AC treatment in mouse eyes and hTM cells. a Cryosections of anterior segments from PBS- (left) and 5-ACtreated (right) eyes were immunostained against THBS1 (green). Nuclei were labeled with DAPI (blue). THBS1 expression in the TM (indicated by yellow arrows) increased after 5-AC treatment when compared to PBS-treated eyes. See also Supplementary Fig. 1. Images are representative of 3 individual mice and were taken using identical settings. Scale bar = 50 μm. CB: ciliary body; TM: trabecular meshwork; SC: Schlemm's canal. b Relative quantification of real time-quantitative polymerase chain reaction (RT-qPCR) showed that 2-day treatment of 5-AC significantly induced THBS1 gene expression in hTM cells when compared to vehicle-control (n = 3 individual cell strains). For each biological replicate (n), the data point represents the average of three technical replicates of each PCR reaction. Data are represented as mean \pm SEM. *P < 0.05 (Student's t test).



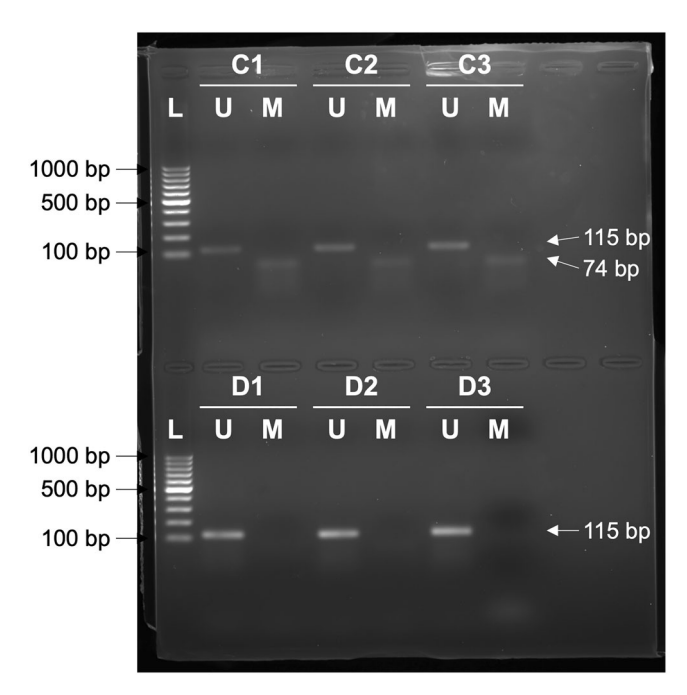


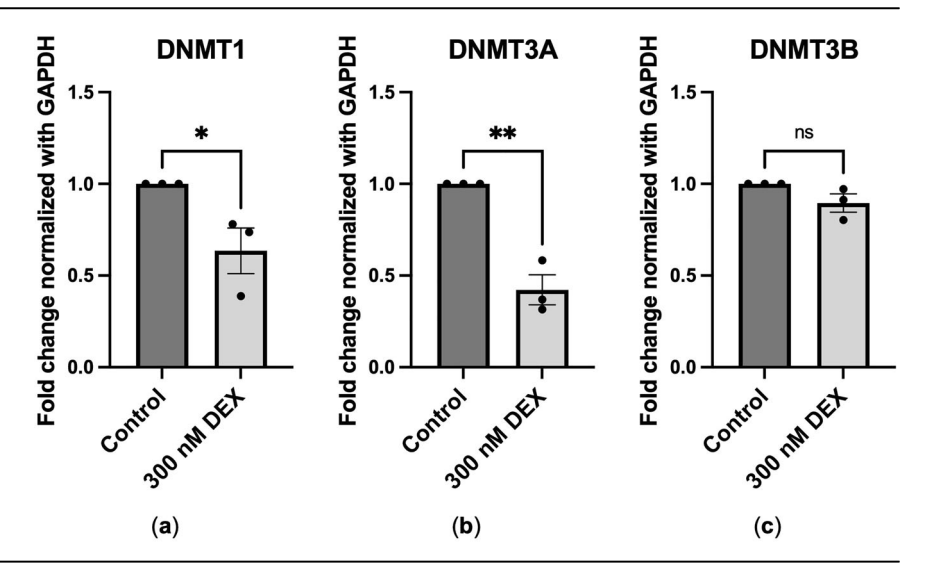
Fig. 4 | Analysis of methylation status of THBS1 promoter in DEX- and vehicle-control hTM cells detected by MSP. Genomic DNA was bisulfite-treated and amplified with a primer set specifically designed for the *THBS1* promoter. MSP results of 3 individual replicates of DEX- (D1-3) and vehicle-control (C1-3) hTM cells are shown. Only unmethylated promoter DNA was detected in samples from DEX treated cells, whereas in control cells both methylated and unmethylated DNA were detected. The original blot is presented in Supplementary Fig. 2C: vehicle-control; D: DEX-treated; L: DNA ladder; M: methylated; U: unmethylated.

sequencing (WGBS) with DEPseq PE100 platforms (BGI, Shenzhen, China). We obtained more than 1 billion clean reads and 100 Gb clean bases from each replicate, after filtering adaptor sequences and low-quality reads. Total reads were mapped to the reference genome using BSMAP, with mapping rates higher than 81% for individual replicates.

In general, methylation occurs at CG, CHG, and CHH (H = A, C, or T) nucleotides of genes. The percentage of methylated cytosines varied according to the local sequence context (C, CG, CHG, and CHH) and the additional treatment (DEX) provided. We found that DEX-treated hTM cells had generally more methylated reads at 2-kb upstream of transcription start site (Up2k) region and CpG islands (CpGIs) than vehicle-control hTM cells, especially at mCG contexts (Fig. 6a; Supplementary Table 1). Up2k regions are the promoter regions at 2,000 bp before the transcription start site of the gene. CpGIs are mainly located in promoter regions of genes and important for epigenetic regulation of gene expression.

A total of 11,644 differentially methylated genes (DMGs) were identified in DEX-treated hTM cells when compared to the vehicle-control, including 4,764 hypomethylated genes and 6,880 hypermethylated (Supplementary Data 1). Of note, based on the positive delta beta ($\Delta\beta$) value, THBS1 was identified as a directionally hypomethylated gene in the WGBS screen. To select biologically meaningful genes in response to DEX treatment, we integrated the lists of genes obtained from WGBS in this study and our published list from mass spectrometry¹⁷. We selected 443 DMGs with corresponding changes in protein expression, including 157 hypomethylated genes and 286 hypermethylated (Supplementary Table 2). THBS1 was identified in this list with matching regulation of methylation and increased protein abundance (approximately 2-fold upregulated versus vehicle-control). To investigate the biological functions of DMGs, Kyoto Encyclopedia of Genes and Genomes (KEGG) pathway enrichment and Gene Ontology (GO) analysis was performed. DMGs belonged mainly to metabolic pathways in the KEGG pathway analysis (Fig. 6b; Supplementary Table 3) and to pathways of transport and cellular localization in GO analysis (Fig. 6c; Supplementary Table 4). Cellular component and molecular function analysis found that DMGs were mainly confined in extracellular and intracellular components, including focal adhesion assemblies, and were

Fig. 5 | DEX downregulated the gene expression of *DNMT1* and *DNMT3A*, but not *DNMT3B*, in hTM cells. RT-qPCR showed that 2-day treatment of 5-AC significantly reduced the gene expression of (a) DNMT1 and (b) DNMT3A, but not (c) DNMT3B, in hTM cells when compared to vehicle-control (n=3 individual cell strains). For each biological replicate (n), the data point represents the average of three technical replicates of each PCR reaction. Data are represented as mean \pm SEM. *P < 0.05 or **P < 0.01 (Student's t test).



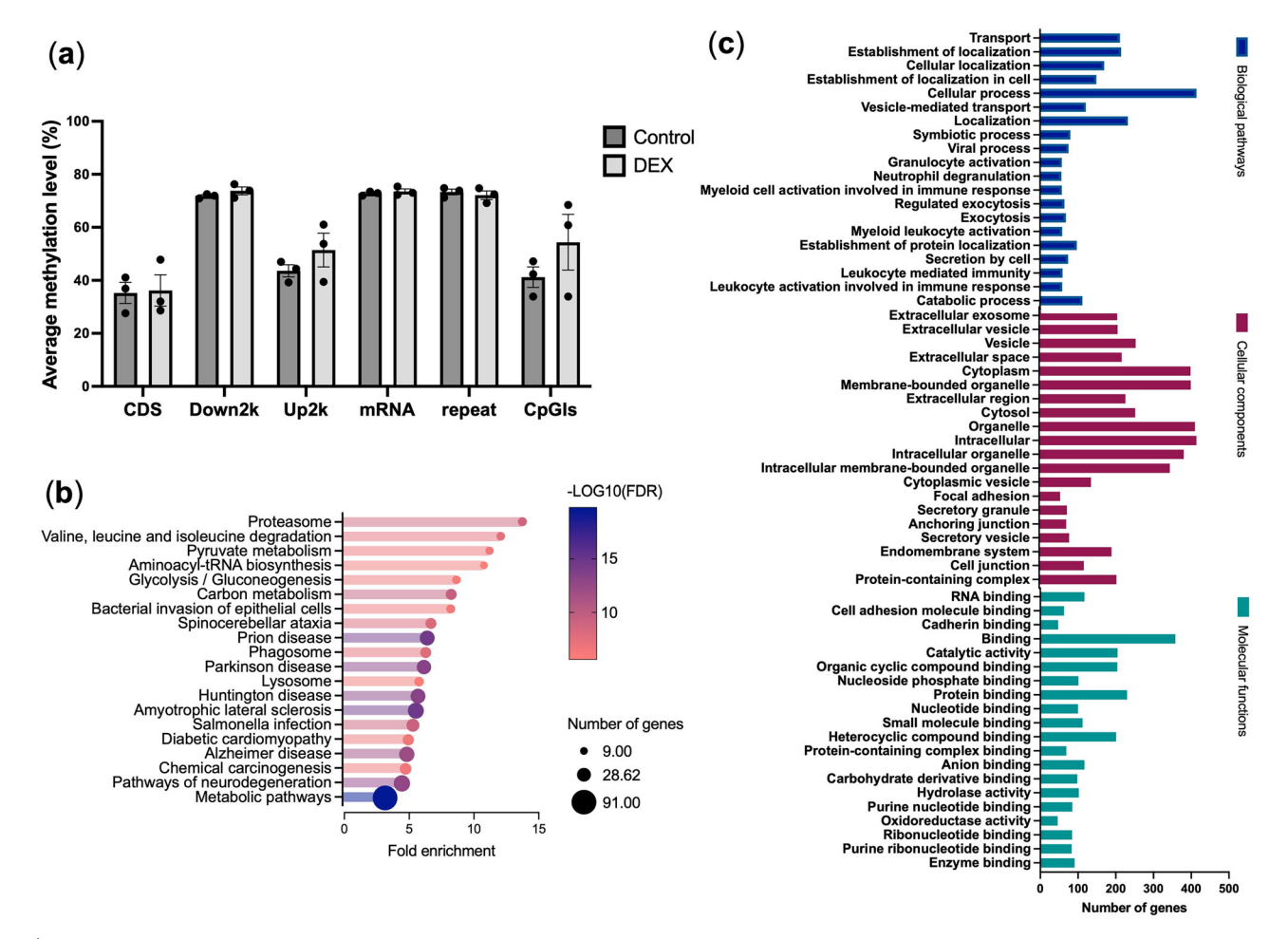


Fig. 6 | DEX induced DNA methylation changes in hTM cells. a At mCG contexts, DEX-treated hTM cells had generally more methylated reads at 2-kb upstream of transcription start site (Up2k) region and CpG islands (CpGIs) than vehicle-control. See also Supplementary Table 1. CDS: coding sequences; Down2k: 2-kb downstream of transcription start site; Up2k: 2-kb upstream of transcription start site; CpGIs: CpG islands. b KEGG pathway enrichment of DMGs is shown, displaying the top 20 pathways. The size of each circle

represents numbers of genes within each pathway and the color represents the false discovery rate. See also Supplementary Table 3. FDR: false discovery rate. c GO analysis of DMGs in terms of biological process (blue), cellular component (red) and molecular functions (green) is shown, displaying the top 20 processes or pathways. The y-axis represents 3 domains of GO while x-axis represents the gene numbers within each pathway and processes. See also Supplementary Table 4.

involved in binding between biomolecules, including cell adhesion molecules and cadherins (Fig. 6c), which may promote interaction between cells, or between cells and ECM, and ECM remodeling. The results link DEX induced changes in DNA methylation to changes in expression of proteins that are relevant for ECM remodeling.

In our previous study, we investigated the effects of 2 corticosteroids, DEX and PRED, on protein expression in hTM cells. We short-listed 20 proteins that were regulated in common by both DEX and PRED¹⁷. When we compared the shortlist and the selected lists of DMGs with corresponding changes (log2 fold-change, Log2FC) in protein expression (Supplementary Table 3), we found 3 significantly hypomethylated and upregulated genes (COL8A1, $\Delta\beta=0.107$, Log2FC=0.688; FLNB, $\Delta\beta=0.178$, Log2FC=0.896; THBS1, $\Delta\beta=0.177$, Log2FC=1.169) and 2 significantly hypermethylated and downregulated genes (SERPINE1, $\Delta\beta=-0.182$, Log2FC=-0.771; SERPINE2, $\Delta\beta=-0.185$, Log2FC=-1.229). All these DMGs encode proteins involved in ECM remodeling, further supporting that DEX alters DNA methylation to regulate the expression of ECM proteins for ECM remodeling.

Discussion

DNA methylation plays an important role in the pathophysiology of many diseases, including glaucoma. In this study, we demonstrated that DNA methylation inhibitors elevated IOP in vivo, reduced outflow facility ex vivo and upregulated THBS1 protein levels both in vivo and in vitro. Likewise, we showed that DEX resulted in DNA hypomethylation at THBS1 promoter region, consistent with our previous findings that DEX upregulated THBS1 in hTM cells. ^{15,17} and present findings that DEX induced a downregulation of DNMTs in hTM cells.

While the exact role of THBS1 in glaucoma remains incompletely characterized, the literature strongly points to increased THBS1 expression may lead to reduced aqueous humor flow and increased IOP. THBS1 expression is increased in glaucoma in the plasma^{30,31}, TM^{15,32}, ocular fibroblasts³³ and the optic nerve head³⁴ in humans. THBS1 level in aqueous humor of primary angle-closure glaucoma patients with negative outcome following trabeculectomy is significantly higher than patients with positive outcome³⁵. THBS1 missense alleles might lead to an unusual buildup of THBS1 assembling with other ECM proteins and increase the risk of primary congenital glaucoma due to the elevated IOP, reduced aqueous outflow and retinal ganglion cell loss induced³⁶⁻³⁸. Conversely, THBS1-null mice have a lower IOP when compared with the wild-type control mice³⁹. Downregulation of THBS1 by siRNA and treatment with an inhibitory peptide increased the outflow facility of mouse eyes ex vivo²², strongly suggesting THBS1 reduces aqueous flow and increases IOP. Prolonged administration of corticosteroids, such as DEX, is known to lead to increased IOP and increase the risk of glaucoma in humans^{32,40,41} and animals including mice and sheep^{42–46}. DEX also induces global changes in DNA methylation and gene expression in hTM and retinal pigment epithelium cells^{23,47}. Our current findings suggest that DEX reduces outflow facility and increases the risk of glaucoma in part by inhibiting DNA methylation of the THBS1 promoter region and stimulating THBS1 gene and protein expression. The effect on the THBS1 promoter region may in part be mediated through DEX-induced downregulation of DNMT expression (Fig. 7).

Besides THBS1, our WGBS results showed that DEX also induced hypomethylation of TGFB1 (Supplementary Table 2), collagen type VIII, alpha 1 (COL8A1, Supplementary Table 2) and filamin B (FLNB, Supplementary Table 2), which may induce their protein expression. TGFB1 is elevated in plasma³¹, aqueous humor^{48,49} and TM cells from glaucoma patients⁵⁰. TGFB1 treatment induced the expression of proteins involved in ECM remodeling and cytoskeletal interactions^{51–53}, elevated IOP⁵² and reduced outflow facility⁵⁴ in perfused human anterior segments. On the other hand, DEX-induced hypomethylation and upregulation of THBS1 may activate TGFB1^{20,55} and sequentially the TGFB signaling pathways to increase ECM accumulation and IOP.

Bachman et al. ⁵⁶ has demonstrated that DEX induced the expression of COL8A1 and FLNB in hTM cells, which is in agreement with our findings that DEX induced a hypomethylation (Supplementary Table 2) and gene expression (Supplementary Fig. 3) of *COL8A1* and *FLNB*. COL8A1 is network-forming collagen involved in ECM and its deficiency in mouse eye caused deeper anterior chamber and thinning of corneal stroma and Descemet membrane⁵⁷, indicating that COL8A1 may be responsible for development of anterior chamber and cornea. COL8A1 may regulate TGFB signaling pathway^{58,59} and modulate the function TGFB1⁶⁰ while TGFB1 may induce COL8A1 expression^{61,62}.

FLNB is a cytoplasmic actin-binding protein which plays an important role in actin cytoskeleton contributing to the formation of highly cross-linked actin networks (CLANs) at $\rm TM^{63}$. DEX-induced expression of FLNB may cause reorganization of CLANs at $\rm TM^{51,64}$, affecting the overall contractility $\rm ^{65}$ and outflow facility resistance $\rm ^{66}$. Our results suggested that DEX induction of COL8A1 and FLNB may lead to remodeling of ECM and CLANs, affecting the IOP and outflow facility.

Altogether, our results suggested that DEX induced hypomethylation of THBS1, TGFB1, COL8A1 and FLNB, which may induce their protein expression. THBS1, TGFB1 and COL8A1 are involved in the TGFB pathway while FLNB is involved in CLANs formation. The activation of these bioprocesses may lead to the remodeling of ECM and the alteration of IOP and outflow facility. However, further studies are needed to confirm the relationship between these proteins in DEX-treated hTM cells.

This study has potential limitations. Our findings demonstrated that DEX induced hypomethylation and upregulation of THBS1 in hTM cells, which may promote TGFB activation ECM remodeling. However, mouse models were adapted to study the effects of DNA methylation inhibitors on outflow facility and IOP regulation. Mouse models are a common and valuable platform for exploring the pathophysiology of human diseases and potential drug candidates in a wide variety of researches, including ocular research in view of several ocular anatomical and physiological similarities between humans and mice, such as the conventional outflow pathway^{27,28}. However, there are nonnegligible differences between the two species, particularly in genetics, physiology and immunology, might limit the ability of mouse models to recapitulate critical human disease pathophysiology and therapeutic responses, and the significance of data interpretation.

Our study also indicates that THBS1 might be a potential therapeutic target to control DEX-induced ocular hypertension. A selective THBS1 antagonist which impairs THBS1 function or inhibits THBS1-mediated activation of TGFB pathway might be a possible direction to be examined in the future. In addition, understanding the molecular mechanism of how DEX regulates the expression of THBS1 could also help establishing new therapeutic strategies to control DEX-induced ocular hypertension.

In conclusion, we have demonstrated that THBS1 protein expression can be increased by reducing the methylation status of the promoter region in the *THBS1* gene and that these changes are associated with reduced outflow facility ex vivo and increased IOP in vivo. In addition, we have shown in hTM cells that DEX reduces methylation of the *THBS1* promoter region, and this change is consistent with DEX-mediated increases in THBS1 protein levels²². DEX-mediated changes in methylation status and protein expression affected, among others, proteins in the cellular localization categories of "endomembrane system" and "focal adhesion" and in the molecular functions categories of "binding" and "cell adhesion molecule binding", which is consistent with the findings of increased ECM deposition in glaucoma and DEX-mediated remodeling of the filamentous actin network in hTM cells²².

Methods

Animals

All the procedures were approved by the Animal Subjects Ethics Sub-Committee of the Hong Kong Polytechnic University (ASESC Case no.: 21-22/89-SO-R-HMRF). All experiments were also performed in compliance with the Guide for the Care and Use of Laboratory Animals published by the National Institutes of Health, the ARVO Statement for the Use of Animals

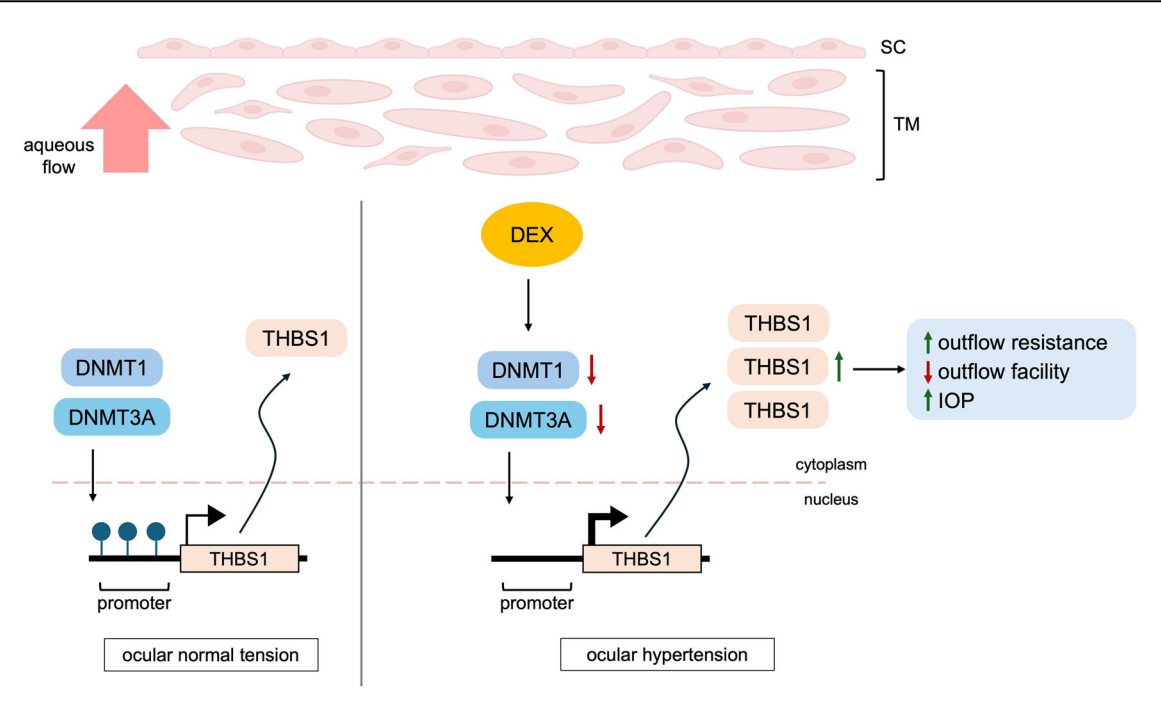


Fig. 7 | Proposed mechanism of DEX-induced ocular hypertension and POAG. DEX induces epigenetic alterations in hTM affecting the DNA methylation and gene expressions globally. Particularly, DEX induces a DNA hypomethylation at *THBS1* promoter region and this aberrant methylation of *THBS1* is due to the DEX-induced

downregulation of *DNMT*s. The upregulation of THBS1 may promote TGFB activation and ECM remodeling, leading to a reduced outflow facility and elevated IOP. SC: Schlemm's canal; TM: trabecular meshwork.

in Research, and the ARRIVE guidelines. Adult male C57BL/6 J mice (2 to 4 months old, RRID:IMSR_JAX:000664) were housed 2–4 per cage with environmental enrichment in a temperature (22–24 °C) and humidity-controlled (50–65%) room. Mice were maintained on a 12-hour light-dark cycle and provided food (LabDiet Cat# 5053) and water *ad libitum*. All experiments were conducted to minimize pain to the greatest extent and the general health of the animals were closely monitored by measuring their body weights. Any animals with weight loss exceeding 20% of the normal body weight and showed signs of severe pain and distress, infection, or inability to obtain food or water were euthanized humanely. All experiments were conducted in a blinded manner, with the researchers responsible for treatment administration and outcome assessment were unaware of which groups of animals belonged to. We have complied with all relevant ethical regulations for animal use.

Non-invasive measurement of IOP

To study the intervention of DNA methylation inhibitor, 5-AC, a total of 10 mice, 2 to 4 months old, were randomly divided into 2 groups: 5 mice in 5-AC treatment group and 5 mice in PBS control group. IOP was measured by a Tonolab rebound tonometer (Icare, Finland) and all IOP measurements were obtained at a consistent time of day to prevent diurnal variation. 6 measurements indicated as successful by Tonolab were conducted consecutively and the averaged repeated successful measurements were reported as a resulting value by Tonolab. 5 resulting values were obtained, and the highest and the lowest resulting values were excluded. An average of remaining 3 resulting values per mouse eye was reported as a data point. After baseline measurement of IOP was established, 1 mouse eye was randomly selected for the topical application of 5-AC (50 µM, Sigma-Aldrich Cat# 855049) or PBS (Gibco Cat# 18912014) thrice a day for 14 days while another eye was left untreated as control. The researchers in charge were masked to the group allocation for topical administration and IOP measurements during the study. The IOP measurements were performed every 2 days in awake mice. Each animal was assigned a random number within the subgroup for longitudinal data collection and IOP measurement order was randomized every 2 days. Random numbers were generated using the standard = RAND() function in Microsoft Excel. The sample size calculation was based on previous studies. The primary outcome of this study was changes in IOP after topical administration of 5-AC or PBS. The power of the experiment was set to 80% to detect a 2-mmHg difference in IOP. A total of 5 mice per group were considered necessary. No unexpected adverse events happened, and no animals were excluded. Comparisons between 5-AC- and PBS-treated groups were conducted.

Measurement of outflow facility

Perfusion of ex vivo mouse eyes was performed using 2 to 4 months old male C57BL/6 J mice. A total of 21 mice were randomly divided into 2 groups: 13 mice in 5-AC group and 8 mice in 5-aza-dC group. Sample size calculation was based on our previous published data using the same perfusion system and mouse strain²². The experiment was performed at 37 °C. Throughout the experiment, ex vivo mouse eyes were continuously perfused with HEPES buffered Ringer's solution containing 113 mM NaCl (Sigma-Aldrich Cat# S7653), 4.56 mM KCl (Sigma-Aldrich Cat# P5405), 21 mM NaHCO₃ (Sigma-Aldrich Cat# S5761), 0.6 mM MgSO₄·7H₂O (Sigma-aldrich Cat# 63138), 7.5 mM D-glucose (Sigma-Aldrich Cat# G5767), 1 mM Re-glutathione (Sigma-Aldrich Cat# G4251), 1 mM Na₂HPO₄·12H₂O (Sigma-Aldrich Cat# 71650), 10 mM HEPES (Sigma-Aldrich Cat# H3375), and 1.4 mM CaCl₂·2H₂O (Sigma-Aldrich Cat# 21097), supplemented with either 5-AC (10 µM) or 5-azadC (10 µM, Sigma-Aldrich Cat# A3656) or vehicle control (PBS). For perfusions, the anterior chambers of paired mouse eyes were cannulated by a 33-gauge needle. The needle was connected via pressure tubing to a glass syringe (50 µl; Hamilton) which was placed on a motorized syringe pump (PhD Ultra; Harvard Apparatus, Holliston, MA) under computer control, and a pressure transducer (model 142PC01G; Honeywell). The pressure of the eye was then monitored by the pressure transducer via a 3-way connector connected to the perfusion system. Sequential pressure steps of 4, 8, 12, 16, and 20 mmHg were used. At each pressure step, stable perfusion was obtained for at least 10 min. The outflow facility was then calculated based on the average flow rate calculated from the stable perfusion period at each perfusion pressure. Any traces with aberrant fluctuations, showing signs of blockage in the tubing or needles by air bubbles, or leakage as judged by the masked researchers, were excluded. 1

mouse eyes perfused with 5-AC showed signs of blockage in the needles and were excluded from further analysis.

Immunohistochemistry staining

After 14-day topical application of 5-AC or PBS, moue eyes were carefully enucleated and fixed in 4% paraformaldehyde (Sigma-Aldrich Cat# 158127) at 4 °C overnight. Whole eyes were bisected, and the posterior segments and lenses were removed. The eye cups were collected and immersed in 30% sucrose at 4 °C overnight. The eyes were embedded in optimal cutting temperature and cryosectioned as 10 μm-thick sections using a cryostat (Leica). Cryosections were immunostained with rabbit anti-THBS1 anti-body (1:100, Abcam Cat# ab85762, RRID:AB_10674322) The secondary antibody was Goat anti-Rabbit IgG (H + L) Cross-Adsorbed Secondary Antibody, Alexa Fluor™ 594 (1:100, Invitrogen Cat# A-11012, RRI-D:AB_2534079) and nuclei were stained with SlowFade™ Diamond Antifade Mountant with DAPI (Invitrogen Cat# S36964). All images were captured using Zeiss LSM 800 Confocal Microscope (Zeiss) and collected at identical intensity and gain settings for all sections.

Primary hTM cell culture

The isolation of hTM cells was performed as described in previous studies 67,68 and authenticated according to consensus recommendations 69 . The hTM cells were plated and incubated at 37 °C with low glucose Dulbecco's modified Eagle's medium (DMEM, low glucose, Invitrogen Cat# 11885076) containing 10% fetal bovine serum (FBS, Invitrogen Cat# 10082147) until confluent and subsequently maintained in low glucose DMEM medium containing 1% FBS for at least a week prior to experiments. Confluent monolayers of hTM cells were either treated with corticosteroid DEX (300 nM, Sigma-Aldrich Cat# D2915) for 7 days or DNA methylation inhibitor 5-AC (0.5-1 μ M) for 2 days, together with corresponding vehicles, and the cells were collected for subsequent assays.

MSP

Genomic DNA was extracted from hTM cells using the DNeasy Blood and Tissue kit (Qiagen Cat# 69504) and modified using the EZ DNA Methylation Bisulfite kit (Zymo Research Cat# D5001), according to the manufacturer's protocols. The methylation status of THBS1 promoter was evaluated using the primers specific for methylated (forward: 5'-GCGAGCGTTTTTTTAAAAGTGC-3'; reverse: 5'-TAAACTCGCAAAC CAACTCG-3') and unmethylated THBS1 (forward: 5'-GAATGTGAGT GTTTTTTTAAAAGTGTG-3'; reverse: 5'-CCTAAACTCACAAACCAA CTCAA-3'), originally designed and reported by Herrera-Goepfert et al. ⁷⁰. The bisulfite-treated DNA was amplified using Premix Taq HS kit (TaKaRa Bio Inc. Cat# R028A). The thermocycling conditions were as follows: 95 °C for 12 min; 45 cycles of (95 °C for 30 seconds, 55 °C for 30 seconds, and 72 °C for 30 seconds), and 72 °C for 10 min. PCR products were analysed on 2% agarose gels and visualized under UV light.

RT-aPCR

The total RNA of hTM cells was extracted and quantified using the RNeasy Micro Kit (Qiagen Cat# 74004). Reverse transcription of mRNA to cDNA was performed using the High-Capacity cDNA Reverse Transcription Kit (Thermo Fisher Scientific Cat# 4368813), followed by qPCR using the LightCycler 480 SYBR Green I Master (Roche Applied Science Cat# 100099593) with primers specific for the target genes: COL8A1 (forward: 5'-GAAATTCAACCGGCGCCAAG-3'; reverse: 5'-TATCCCTGTGGCC CTGGTTT-3'), FLNB (forward: 5'- AGCGATCCCAGTGCAGTTTG-3'; reverse: 5'- TCGGAGCACTCGATTTTGGC-3'), TPM (forward: 5'-GTTCATCCACTCTGCCTGCT-3'; reverse: 5'- CAGTGTGTGCCT GGCTCTAA-3'), TUBA4A (forward: 5'- GATGCCCAGTGACAA-GACCA-3'; reverse: 5'- GCAGCATCCTCTTTCCCAGT-3'), COLGALT1 (forward: 5'- GCAGGCAGAGGTTCAGATGT-3'; reverse: 5'- GTGCTT CACCATGACCTCCA-3'), DNMT1 (forward: 5'-AGACTACGCGA-GATTCGAGTC-3'; reverse: 5'-TTGGTGGCTGAGTAGTAGAGG-3'), DNMT3A (forward: 5'-GCGGCGAGAGGACTGGCC-3'; reverse: 5'-

CGGTCCACCTGAATGCCCAA-3'), *DNMT3B* (forward: 5'-AGGGA-GACACCAGGCATCTC-3'; reverse: 5'-AGCTTAGCAGACTGGACA CC-3'), *THBS1* (forward: 5'-CGTCCTGTTCCTGATGCATG-3'; reverse: 5'-CCAGGAGAGCTTCTTCCACA-3'), and the internal reference gene, *GAPDH* (forward: 5'-GATTTGGTCGTATTGGGCGC-3'; reverse: 5'-TGGACTCCACGACGTACTCA-3'). qPCR was performed in 96-well plates on the ROCHE LightCycler 480 (Roche Applied Science). In each 10 µl reaction, 1 × Taq PCR Master Mix, 2 µl of cDNA template and 10 µM primers (forward and reverse primers, respectively) were used. The thermal cycling conditions were 95 °C for 5 min, followed by 40 cycles of (95 °C for 30 seconds, 61 °C for 30 seconds, and 72 °C for 30 seconds). A melting-curve analysis was performed to rule out primer–dimer formation and non-specific product amplification. A negative control sample without a template was included in each plate. Data were analysed using LightCycler software (RRID:SCR_012155).

WGBS

Genomic DNA was extracted from hTM cells using a DNeasy Blood and Tissue kit following the manufacturer's manual, quantified by UV spectroscopy, and then subjected to WGBS analysis (BGI). In brief, BGI first constructed the DNA library by fragmenting DNA by sonication with a Bioruptor (Diagenode), followed by blunt ends formation and methylated adaptor ligation. The ligation products were bisulfite converted and separated on a 2% TAE agarose gel. Fragments were excised from the agarose gels and purified, followed by PCR amplification and cyclization. Finally, the DNA libraries were sequenced on the DNBseq PE100 platform and raw data were filtered to remove adaptor sequences, contamination, and low-quality reads. Clean data obtained were mapped to the reference genome using BSMAP software (RRID:SCR_005671)⁷¹, followed by removal of duplication reads and merging of mapped results of each library.

The difference in rate of cytosine methylation (mCG, mCHG, mCHH) for a given DNA region was calculated as β -value and compared between DEX- and vehicle-control hTM cells. β -value is the ratio of the number of reads covering a methylated cytosines over the total number of reads covering that cytosines. $\Delta\beta$ is defined as the average β -value of vehicle-control samples minus that of DEX-treated samples. Results with P-value below 0.05 and $\Delta\beta$ ranges from -0.1 to 0.1 are considered statistically significant and differentially methylated. To identify their biological functions, the DMGs were analysed for GO and KEGG enrichment using the Shiny Go 0.77 tool (RRID:SCR_019213)^72, with a false discovery rate below 0.05 and a P-value below 0.05 as cut-off values. The WGBS data discussed in this publication have been deposited in NCBI's Gene Expression Omnibus (RRID:SCR_005012) and are accessible through GEO Series accession number GSE271511.

Statistics and reproducibility

Statistical analyses used for each experiment are detailed in the figure legends and were calculated using GraphPad Prism version 10.2.3 (RRID:SCR_000306). For comparisons of any two data groups of different samples, p values were calculated using unpaired student's t test. For comparison of multiple parallel data groups, p values were calculated with two-way repeated measures ANOVA followed by Bonferroni's multiple comparisons test. Number (n) represents biological replicate, i.e., individual mouse eye or cell strain. Error bars indicate SEM unless otherwise specified. A p-value below 0.05 was considered statistically significant. *P < 0.05; **P < 0.01; ***P < 0.001.

No formal protocol including the research question, key design features, and analysis plan was registered before the study. Further information on research design is available in the Nature Portfolio Reporting Summary linked to this article.

Reporting summary

Further information on research design is available in the Nature Portfolio Reporting Summary linked to this article.

Data availability

The source data for graphs analyzed in the study are available in the Supplementary Data 2. The dataset produced in this study is available through Gene Expression Omnibus GSE271511. All other data are available from the corresponding author on reasonable request.

Received: 17 March 2025; Accepted: 2 September 2025; Published online: 06 October 2025

References

- Fuchsjager-Mayrl, G. et al. Ocular blood flow and systemic blood pressure in patients with primary open-angle glaucoma and ocular hypertension. *Invest. Ophthalmol. Vis. Sci.* 45, 834–839 (2004).
- Chen, S. J., Lu, P., Zhang, W. F. & Lu, J. H. High myopia as a risk factor in primary open angle glaucoma. *Int. J. Ophthalmol.* 5, 750–753 (2012)
- Ha, A., Kim, C. Y., Shim, S. R., Chang, I. B. & Kim, Y. K. Degree of myopia and glaucoma risk: a dose-response meta-analysis. *Am. J. Ophthalmol.* 236, 107–119 (2022).
- 4. Jonas, J. B., Wang, Y. X., Dong, L. & Panda-Jonas, S. High myopia and glaucoma-like optic neuropathy. *Asia Pac. J. Ophthalmol. (Philos.* **9**, 234–238 (2020).
- Marcus, M. W., de Vries, M. M., Junoy Montolio, F. G. & Jansonius, N. M. Myopia as a risk factor for open-angle glaucoma: a systematic review and meta-analysis. *Ophthalmology* 118, 1989–1994 e1982 (2011).
- Kass, M. A., Hart, W. M. Jr., Gordon, M. & Miller, J. P. Risk factors favoring the development of glaucomatous visual field loss in ocular hypertension. Surv. Ophthalmol. 25, 155–162 (1980).
- Medeiros, F. A. et al. Validation of a predictive model to estimate the risk of conversion from ocular hypertension to glaucoma. *Arch. Ophthalmol.* 123, 1351–1360 (2005).
- Ocular Hypertension Treatment Study, G. et al. Validated prediction model for the development of primary open-angle glaucoma in individuals with ocular hypertension. *Ophthalmology* 114, 10–19 (2007).
- Quigley, H. A. et al. Risk factors for the development of glaucomatous visual field loss in ocular hypertension. *Arch. Ophthalmol.* 112, 644–649 (1994).
- Becker, B. & Mills, D. W. Corticosteroids and intraocular pressure. *Arch. Ophthalmol.* 70, 500–507 (1963).
- Bernstein, H. N., Mills, D. W. & Becker, B. Steroid-induced elevation of intraocular pressure. Arch. Ophthalmol. 70, 15–18 (1963).
- Becker, B. & Mills, D. W. Elevated intraocular pressure following corticosteroid eye drops. *JAMA* 185, 884–886 (1963).
- Goldmann, H. Cortisone glaucoma. Arch. Ophthalmol. 68, 621–626 (1962).
- Garnock-Jones, K. P. Ripasudil: first global approval. *Drugs* 74, 2211–2215 (2014).
- Flugel-Koch, C., Ohlmann, A., Fuchshofer, R., Welge-Lussen, U. & Tamm, E. R. Thrombospondin-1 in the trabecular meshwork: localization in normal and glaucomatous eyes, and induction by TGFbeta1 and dexamethasone in vitro. Exp. Eye Res 79, 649–663 (2004).
- Tripathi, B. J., Tripathi, R. C., Yang, C., Millard, C. B. & Dixit, V. M. Synthesis of a thrombospondin-like cytoadhesion molecule by cells of the trabecular meshwork. *Invest. Ophthalmol. Vis. Sci.* 32, 181–188 (1991).
- Shan, S. W. et al. New Insight of Common Regulatory Pathways in Human Trabecular Meshwork Cells in Response to Dexamethasone and Prednisolone Using an Integrated Quantitative Proteomics: SWATH and MRM-HR Mass Spectrometry. J. Proteome Res. 16, 3753–3765 (2017).
- Kaneko, Y. et al. Effects of K-115 (Ripasudil), a novel ROCK inhibitor, on trabecular meshwork and Schlemm's canal endothelial cells. Sci. Rep. 6, 19640 (2016).

- Murphy-Ullrich, J. E., Schultz-Cherry, S. & Hook, M. Transforming growth factor-beta complexes with thrombospondin. *Mol. Biol. Cell* 3, 181–188 (1992).
- Crawford, S. E. et al. Thrombospondin-1 is a major activator of TGFbeta1 in vivo. Cell 93, 1159–1170 (1998).
- Murphy-Ullrich, J. E. Thrombospondin 1 and its diverse roles as a regulator of extracellular matrix in fibrotic disease. *J. Histochem Cytochem* 67, 683–699 (2019).
- Shan, S. W. et al. Thrombospondin-1 mediates Rho-kinase inhibitorinduced increase in outflow-facility. *J. Cell Physiol.* 236, 8226–8238 (2021).
- Matsuda, A. et al. DNA methylation analysis of human trabecular meshwork cells during dexamethasone stimulation. *Invest Ophthalmol. Vis. Sci.* 56, 3801–3809 (2015).
- Hermann, A., Goyal, R. & Jeltsch, A. The Dnmt1 DNA-(cytosine-C5)methyltransferase methylates DNA processively with high preference for hemimethylated target sites. *J. Biol. Chem.* 279, 48350–48359 (2004).
- 25. JÜNEMANN, A. et al. Genomic (epigenetic) DNA methylation in patients with open-angle glaucoma. *Acta Ophthalmologica* **87**, 0–0 (2009).
- Cai, J. et al. Differential DNA methylation patterns in human Schlemm's canal endothelial cells with glaucoma. *Mol. Vis.* 26, 483–493 (2020).
- McDowell, C. M. et al. Consensus recommendation for mouse models of ocular hypertension to study aqueous humor outflow and its mechanisms. *Invest Ophthalmol. Vis. Sci.* 63, 12 (2022).
- Vézina, M. in Assessing Ocular Toxicology in Laboratory Animals (eds Andrea B. Weir & Margaret Collins) 1-21 (Humana Press, 2013).
- Hamidi, T., Singh, A. K. & Chen, T. Genetic alterations of DNA methylation machinery in human diseases. *Epigenomics* 7, 247–265 (2015).
- Kuchtey, J. et al. Elevated transforming growth factor beta1 in plasma of primary open-angle glaucoma patients. *Invest. Ophthalmol. Vis.* Sci. 55, 5291–5297 (2014).
- 31. Murphy-Ullrich, J. E. & Downs, J. C. The Thrombospondin1-TGF-beta Pathway and Glaucoma. *J. Ocul. Pharm. Ther.* **31**, 371–375 (2015).
- Yan, J. et al. Integrative transcriptomic and proteomic analysis reveals CD9/ITGA4/PI3K-Akt axis mediates trabecular meshwork cell apoptosis in human glaucoma. J. Cell Mol. Med. 24, 814–829 (2020).
- Roodnat, A. W. et al. Genome-wide RNA sequencing of ocular fibroblasts from glaucomatous and normal eyes: Implications for glaucoma management. PLoS One 19, e0307227 (2024).
- Kirwan, R. P., Wordinger, R. J., Clark, A. F. & O'Brien, C. J. Differential global and extra-cellular matrix focused gene expression patterns between normal and glaucomatous human lamina cribrosa cells. *Mol. Vis.* 15, 76–88 (2009).
- 35. Zhu, J. D., Xie, L. L., Li, Z. Y. & Lu, X. H. The prognosis of trabeculectomy in primary angle-closure glaucoma patients. *Int J. Ophthalmol.* **12**, 66–72 (2019).
- Fu, H. et al. Thrombospondin 1 missense alleles induce extracellular matrix protein aggregation and TM dysfunction in congenital glaucoma. J. Clin. Invest. 132 (2022). https://doi.org/10.1172/ JCI156967
- Somarajan, B. I. et al. Analysis of early-onset glaucoma genes in primary congenital glaucoma patients residing in North India identifies an additional case with THBS1 Arg1034Cys. *Ophthalmic Genet.* 1-5 (2025).
- Wirtz, M. K. et al. Identification of missense extracellular matrix gene variants in a large glaucoma pedigree and investigation of the N700S thrombospondin-1 variant in normal and glaucomatous trabecular meshwork cells. *Curr. Eye Res.* 47, 79–90 (2022).
- Haddadin, R. I. et al. Thrombospondin-1 (TSP1)-null and TSP2-null mice exhibit lower intraocular pressures. *Invest Ophthalmol. Vis. Sci.* 53, 6708–6717 (2012).

- Clark, A. F. Basic sciences in clinical glaucoma: steroids, ocular hypertension, and glaucoma. *J. Glaucoma* 4, 354–369 (1995).
- Clark, A. F. & Wordinger, R. J. The role of steroids in outflow resistance. Exp. Eye Res. 88, 752–759 (2009).
- Whitlock, N. A., McKnight, B., Corcoran, K. N., Rodriguez, L. A. & Rice, D. S. Increased intraocular pressure in mice treated with dexamethasone. *Invest. Ophthalmol. Vis. Sci.* 51, 6496–6503 (2010).
- Patel, G. C. et al. Dexamethasone-induced ocular hypertension in mice: effects of myocilin and route of administration. *Am. J. Pathol.* 187, 713–723 (2017).
- Overby, D. R. et al. Ultrastructural changes associated with dexamethasone-induced ocular hypertension in mice. *Invest Ophthalmol. Vis. Sci.* 55, 4922–4933 (2014).
- Zode, G. S. et al. Ocular-specific ER stress reduction rescues glaucoma in murine glucocorticoid-induced glaucoma. *J. Clin. Invest.* 124, 1956–1965 (2014).
- Gerometta, R., Podos, S. M., Danias, J. & Candia, O. A. Steroidinduced ocular hypertension in normal sheep. *Invest Ophthalmol. Vis.* Sci. 50, 669–673 (2009).
- Liu, W. et al. Epigenetic alterations associated with dexamethasone sodium phosphate through DNMT and TET in RPE cells. *Mol. Vis.* 27, 643–655 (2021).
- Agarwal, P., Daher, A. M. & Agarwal, R. Aqueous humor TGF-beta2 levels in patients with open-angle glaucoma: A meta-analysis. *Mol. Vis.* 21, 612–620 (2015).
- Inatani, M. et al. Transforming growth factor-beta 2 levels in aqueous humor of glaucomatous eyes. *Graefes Arch. Clin. Exp. Ophthalmol.* 239, 109–113 (2001).
- Tovar-Vidales, T., Clark, A. F. & Wordinger, R. J. Transforming growth factor-beta2 utilizes the canonical Smad-signaling pathway to regulate tissue transglutaminase expression in human trabecular meshwork cells. Exp. Eye Res. 93, 442–451 (2011).
- Bollinger, K. E. et al. Quantitative proteomics: TGFbeta(2) signaling in trabecular meshwork cells. *Invest Ophthalmol. Vis. Sci.* 52, 8287–8294 (2011).
- Fleenor, D. L. et al. TGFbeta2-induced changes in human trabecular meshwork: implications for intraocular pressure. *Invest Ophthalmol.* Vis. Sci. 47, 226–234 (2006).
- Fuchshofer, R., Welge-Lussen, U. & Lutjen-Drecoll, E. The effect of TGF-beta2 on human trabecular meshwork extracellular proteolytic system. Exp. Eye Res. 77, 757–765 (2003).
- 54. Gottanka, J., Chan, D., Eichhorn, M., Lutjen-Drecoll, E. & Ethier, C. R. Effects of TGF-beta2 in perfused human eyes. *Invest Ophthalmol. Vis. Sci.* **45**, 153–158 (2004).
- 55. Murphy-Ullrich, J. E. & Poczatek, M. Activation of latent TGF-beta by thrombospondin-1: mechanisms and physiology. *Cytokine Growth Factor Rev.* **11**, 59–69 (2000).
- Bachman, W. et al. Glucocorticoids preferentially influence expression of nucleoskeletal actin network and cell adhesive proteins in human trabecular meshwork cells. Front Cell Dev. Biol. 10, 886754 (2022).
- Hopfer, U. et al. Targeted disruption of Col8a1 and Col8a2 genes in mice leads to anterior segment abnormalities in the eye. FASEB J. 19, 1232–1244 (2005).
- Feng, H., Jiang, C., Xu, D. & Cang, S. COL8A1 is a prognostic-related biomarker and correlated with immune infiltration in gastric cancer. *Clin. Surg. Oncol.* 2, 100027 (2023).
- 59. Zhou, J. et al. Upregulation of COL8A1 indicates poor prognosis across human cancer types and promotes the proliferation of gastric cancer cells. *Oncol. Lett.* **20**, 34 (2020).
- Loeffler, I., Hopfer, U., Koczan, D. & Wolf, G. Type VIII collagen modulates TGF-beta1-induced proliferation of mesangial cells. *J. Am. Soc. Nephrol.* 22, 649–663 (2011).

- Boguslawska, J. et al. Expression of genes involved in cellular adhesion and extracellular matrix remodeling correlates with poor survival of patients with renal cancer. *J. Urol.* 195, 1892–1902 (2016).
- Saadat, S. et al. Pivotal role of TGF-beta/Smad signaling in cardiac fibrosis: non-coding RNAs as Effectual Players. Front. Cardiovasc. Med. 7, 588347 (2020).
- Clark, R. et al. Comparative genomic and proteomic analysis of cytoskeletal changes in dexamethasone-treated trabecular meshwork cells. *Mol. Cell Proteom.* 12, 194–206 (2013).
- Clark, A. F. et al. Glucocorticoid-induced formation of cross-linked actin networks in cultured human trabecular meshwork cells. *Invest Ophthalmol. Vis. Sci.* 35, 281–294 (1994).
- O'Brien, E. T., Perkins, S. L., Roberts, B. C. & Epstein, D. L. Dexamethasone inhibits trabecular cell retraction. *Exp. Eye Res.* 62, 675–688 (1996).
- Wang, K. et al. The relationship between outflow resistance and trabecular meshwork stiffness in mice. Sci. Rep. 8, 5848 (2018).
- Snyder, R. W., Stamer, W. D., Kramer, T. R. & Seftor, R. E.
 Corticosteroid treatment and trabecular meshwork proteases in cell and organ culture supernatants. *Exp. Eye Res.* 57, 461–468 (1993).
- Stamer, W. D., Seftor, R. E., Williams, S. K., Samaha, H. A. & Snyder, R. W. Isolation and culture of human trabecular meshwork cells by extracellular matrix digestion. *Curr. Eye Res.* 14, 611–617 (1995).
- Keller, K. E. et al. Consensus recommendations for trabecular meshwork cell isolation, characterization and culture. *Exp. Eye Res.* 171, 164–173 (2018).
- Herrera-Goepfert, R. et al. Methylation of DAPK and THBS1 genes in esophageal gastric-type columnar metaplasia. World J. Gastroenterol. 22, 4567–4575 (2016).
- Xi, Y. & Li, W. BSMAP: whole genome bisulfite sequence MAPping program. BMC Bioinform. 10, 232 (2009).
- Ge, S. X., Jung, D. & Yao, R. ShinyGO: a graphical gene-set enrichment tool for animals and plants. *Bioinformatics* 36, 2628–2629 (2020).
- Edgar, R., Domrachev, M. & Lash, A. E. Gene Expression Omnibus: NCBI gene expression and hybridization array data repository. Nucleic Acids Res. 30, 207–210 (2002).

Acknowledgements

We thank the University Research Facility in Life Sciences, The Hong Kong Polytechnic University, for providing and maintaining the equipment needed for RT-qPCR. We also thank the Centralized Animal Facilities, The Hong Kong Polytechnic University, for providing the animal husbandry service. S.S.S. discloses support for the research of this work from PolyU Internal Grants (1-BD6R, 1-CD65) and Health and Medical Research Fund (08191556, 09200276). C.D. discloses support for the research of this work from the InnoHK initiative of the Innovation and Technology Commission of the Hong Kong Special Administrative Region Government and Health and Medical Research Fund (20212781).

Author contributions

K.Y.C. analysed, interpreted and validated the data, and wrote the original manuscript; W.Y. performed experiments and reviewed the manuscript. C.L. performed experiments; H. Li performed experiments; K.L. performed experiments; H. Lung planned and performed experiments, and reviewed the manuscript; C.T. planned experiments; C.W.D. planned experiments, acquired funding and reviewed the manuscript; W.D.S. planned experiments, contributed resources and reviewed the manuscript; S.S.S. provided supervision, planned experiments, acquired funding, analysed and interpreted the data, and reviewed the manuscript.

Competing interests

The authors declare no competing interests.

Ethics statement

All collaborators of this study have fulfilled all authorship criteria required by Nature Portfolio journal and have been included as authors since their contributions were greatly essential for the design and implementation of this study. Roles and responsibilities were agreed amongst collaborators ahead of this study. This study reports findings that are locally relevant and has been determined in collaboration with local partners. This study was not severely restricted or prohibited in the setting of the researchers, and does not result in stigmatization, incrimination, discrimination or personal risk to participants. Local and regional research relevant to our study was taken into account in citations.

Additional information

Supplementary information The online version contains supplementary material available at https://doi.org/10.1038/s42003-025-08833-y.

Correspondence and requests for materials should be addressed to Samantha Sze-wan Shan.

Peer review information *Communications Biology* thanks Fridolin Langer and the other, anonymous, reviewer(s) for their contribution to the peer review of this work. Primary Handling Editor: Ophelia Bu.

Reprints and permissions information is available at

http://www.nature.com/reprints

Publisher's note Springer Nature remains neutral with regard to jurisdictional claims in published maps and institutional affiliations.

Open Access This article is licensed under a Creative Commons Attribution-NonCommercial-NoDerivatives 4.0 International License, which permits any non-commercial use, sharing, distribution and reproduction in any medium or format, as long as you give appropriate credit to the original author(s) and the source, provide a link to the Creative Commons licence, and indicate if you modified the licensed material. You do not have permission under this licence to share adapted material derived from this article or parts of it. The images or other third party material in this article are included in the article's Creative Commons licence, unless indicated otherwise in a credit line to the material. If material is not included in the article's Creative Commons licence and your intended use is not permitted by statutory regulation or exceeds the permitted use, you will need to obtain permission directly from the copyright holder. To view a copy of this licence, visit http://creativecommons.org/licenses/by-nc-nd/4.0/.

© The Author(s) 2025